

Metabolomics of cerebrospinal fluid reveals changes in the central nervous system metabolism in a rat model of multiple sclerosis

Marek J. Noga · Adrie Dane · Shanna Shi · Amos Attali · Hans van Aken · Ernst Suidgeest · Tinka Tuinstra · Bas Mulwijk · Leon Coulier · Theo Luider · Theo H. Reijmers · Rob J. Vreeken · Thomas Hankemeier

Received: 5 January 2011 / Accepted: 30 March 2011 / Published online: 16 April 2011
© The Author(s) 2011. This article is published with open access at Springerlink.com

Abstract Experimental Autoimmune Encephalomyelitis (EAE) is the most commonly used animal model for Multiple Sclerosis (MS). CSF metabolomics in an acute EAE rat model was investigated using targeted LC–MS and GC–MS. Acute EAE in Lewis rats was induced by co-injection of Myelin Basic Protein with Complete Freund's Adjuvant. CSF samples were collected at two time points: 10 days after inoculation, which was during the onset of the disease, and 14 days after inoculation, which was during the peak of the disease. The obtained metabolite profiles from the two time points of EAE development show profound differences between onset and the peak of

the disease, suggesting significant changes in CNS metabolism over the course of MBP-induced neuroinflammation. Around the onset of EAE the metabolome profile shows significant decreases in arginine, alanine and branched amino acid levels, relative to controls. At the peak of the disease, significant increases in concentrations of multiple metabolites are observed, including glutamine, *O*-phosphoethanolamine, branched-chain amino acids and putrescine. Observed changes in metabolite levels suggest profound changes in CNS metabolism over the course of EAE. Affected pathways include nitric oxide synthesis, altered energy metabolism, polyamine synthesis and levels of endogenous antioxidants.

Marek Noga and Adrie Dane contributed equally to this manuscript.

Electronic supplementary material The online version of this article (doi:10.1007/s11306-011-0306-3) contains supplementary material, which is available to authorized users.

M. J. Noga (✉) · A. Dane · S. Shi · T. H. Reijmers · R. J. Vreeken · T. Hankemeier
Leiden/Amsterdam Center for Drug Research, Leiden University, P.O. Box 9502, 2300, RA, Leiden, The Netherlands
e-mail: m.noga@lacdr.leidenuniv.nl

A. Attali · H. van Aken · E. Suidgeest · T. Tuinstra
Abbott Healthcare Products B.V., Weesp, The Netherlands

B. Mulwijk · L. Coulier
TNO Zeist, Zeist, The Netherlands

A. Dane · S. Shi · L. Coulier · T. H. Reijmers · R. J. Vreeken · T. Hankemeier
Netherlands Metabolomics Centre, Leiden/Amsterdam Center for Drug Research, Leiden University, Leiden, The Netherlands

T. Luider
Erasmus Medical Center, Rotterdam, The Netherlands

Keywords Metabolomics · CSF · Multiple sclerosis · EAE · LC–MS · GC–MS

1 Introduction

Multiple sclerosis (MS) is a chronic demyelinating neurodegenerative central nervous system (CNS) disorder of autoimmune origin affecting over 1 million people worldwide. Development of the disease includes emergence of inflammatory lesions in white matter and dysfunction of neural conductivity. This leads to impairment of sensory and motor functions. Molecular processes associated with the onset and progression of MS and its etiology are still unknown.

Because of obvious ethical and safety constraints, access to human brain and spinal cord system samples is very limited. Therefore in-depth investigation of molecular mechanisms of disorders within CNS is hampered. Biochemistry of CNS activity of affected patients can be monitored only indirectly, using cerebrospinal fluid (CSF)

for diagnostic purposes. Also explorative studies of molecular mechanisms involved in the onset and progression of neurological diseases except for brain tumors are limited to CSF samples. The metabolites present in the CSF represent actual metabolism of CNS and the balance between blood and CSF. Its analysis can be helpful in the determination of markers for neurological disorders. However, sampling human CSF is an invasive procedure, hence access to such samples is much more limited compared to blood or urine. In order to partially avoid these limitations, animal models of neurological diseases have been introduced. An additional major advantage of animal models is less variation between individual animals compared to variation between individuals in clinical cohorts. Therefore the discovery of dominating factors of the onset and progression of the disease is more straightforward. On the other hand, biomarkers discovered by means of animal models may not be relevant for the human situation and such results need to be validated and confirmed using clinical data.

The most commonly used animal model of MS is the experimental autoimmune encephalomyelitis (EAE). The course of EAE resembles the symptoms of MS and can be used to study some aspects of MS interconnected with neuroinflammation and neurodegeneration. In this model, disease is induced by inoculating animal with myelin-specific antigens. This paper describes a study investigating changes in metabolites caused by acute EAE; an autoimmune reaction was provoked using MBP co-injected with an adjuvant containing *Mycobacterium tuberculosis* proteins. In this model, gradual and reversible impairment of motor function is observed, however no clear myelin loss is observed.

Metabolomics, the comprehensive analysis of a wide range of metabolites, provides a novel perspective for the search of new disease biomarkers and drug targets, being an alternative and complementary approach to more established omics techniques such as genomics, transcriptomics or proteomics. Recent progress in metabolomics resulted in an increasing number of metabolomics applications in neurological research. In a recent review, Wishart et al. (2008) summarized the current status of CSF metabolomics reporting 308 metabolites together with their concentrations in CSF. Recent articles investigating CSF metabolome focused on untargeted approaches (Crews et al. 2009; Myint et al. 2009; Carrasco-Pancorbo et al. 2009; Wuolikainen et al. 2009) detecting high number of features. In this article we used a related approach emphasizing targeted metabolomics. We applied two platforms, allowing the fully validated analysis of 39 identified metabolites by LC-MS and 64 identified metabolites by GC-MS, with an overlap of 18 metabolites between both methods.

2 Materials and methods

2.1 Induction of acute EAE in the Lewis rat

Male Lewis rats (Harlan Laboratories B.V., the Netherlands) kept under normal housing conditions with water and food ad libitum, weighing between 175 and 225 g at the start of the experiment, were inoculated on day 0 as previously described (Hendriks et al. 2004). Briefly, a 100 μ l saline based emulsion containing 50 μ l Complete Freund's Adjuvant H37 RA (CFA, Difco Laboratories, Detroit, MI), 500 μ l *Mycobacterium tuberculosis* type H37RA (Difco) and 20 μ g guinea pig myelin basic protein (MBP) was injected subcutaneously in the pad of left hind paw of Isoflurane anaesthetized animals. Next to these MBP challenged rats, referred to as the EAE group, two control groups were included: a group of animals receiving the same emulsion without MBP (CFA group) and a healthy group undergoing anesthesia only (Healthy group, H). Each group consisted of 30 animals. Of each group, half of the animals were sacrificed to collect plasma and CSF on day 10 (day of onset of disease in EAE group) resulting in groups further referred as H₁₀, CFA₁₀ and EAE₁₀, and the other half on day 14 (peak of disease in EAE group)—groups H₁₄, CFA₁₄ and EAE₁₄.

Animals were grouped and housed three per cage and cages were randomized across treatments and disease duration. Disease symptoms and weights of all animals were recorded daily. The following scores for motor dysfunctions were used: 0, healthy animal with normal curling reflex at the tail; 1, paralysis of the tip of the tail; 2, loss of muscle tone at the base of the tail; 3, low posture of hind limbs; 4, instability at hips; 5, partial hind limb paralysis; 6, complete hind limb paralysis; 7, paralysis include midriff; 8, quadriplegia; 9, moribund; 10, death due to EAE. The animal experiments described were approved by the local Ethical Committee for Animal Experiments.

2.2 CSF sampling

On day 10 and 14, animals were euthanized with CO₂/O₂ and the head of the rat was fixed in a holder. Terminal CSF samples were obtained by direct insertion of an insulin syringe needle (Myjector, 29G \times 1/2") via the arachnoid membrane into the Cisterna Magna. For this purpose a skin incision was made followed by a horizontal incision in the *musculus trapezius pars descendens* to reveal the Arachnoid membrane. A maximal volume of 60 μ l was collected per animal. Each sample was centrifuged within 20 min after sampling, for 10 min at 2000 \times g at 4°C. After centrifugation, the supernatants were stored at -80°C for further analysis. Previous experiments have shown that collecting up to 60 μ l using this technique and conditions

provided hemoglobin-free CSF samples measured by ESI-Orbitrap (data not shown). As an additional check, fresh samples, supernatant and pellet size were visually scored for hemolysis and samples were discarded if positive (data not shown). After inspection, samples were aliquoted in volumes of 10 μl for analysis by different analytical platforms.

Due to the disturbed physiological state of animals of full EAE group at day 14 (EAE₁₄), the success rate for CSF sampling for these animals was significantly lower, limiting the number of available samples. From 90 animals used in the experiment, 84 CSF samples were available for the LC-MS platform (11 in group EAE₁₄) and 84 for the GC-MS platform (10 in group EAE₁₄).

2.3 LC-MS/MS method

The LC-MS method employed is targeted to the analysis of primary and secondary amines using AccQ-Tag derivatization. 10 μl of CSF sample was spiked with 10 μl of an internal standard solution containing $^{13}\text{C}^{15}\text{N}$ -labeled amino acids, followed by addition of 100 μl of MeOH for deproteinization. The mixture was vortexed for 10 s and centrifuged at $9400\times g$ for 10 min at 10°C. The supernatant was transferred to a deactivated autosampler vial (Waters) and dried under N_2 . The residue was reconstituted in 80 μl of borate buffer (pH 8.5) vortexed for 10 s and treated with 20 μl of AccQ-TagAQC derivatization reagent (Waters). After keeping the mixture for 10 min at 55°C, the vials were transferred to an autosampler tray and cooled to 10°C until the injection. 1.0 μl of the reaction mixture was injected into the UPLC-MS/MS system.

An ACQUITY UPLC system with autosampler (Waters, Etten-Leur, The Netherlands) was coupled online with a Quattro Premier XE tandem quadrupole mass spectrometer (Waters) operated using Masslynx data acquisition software (version 4.1; Waters). The samples were analyzed by UPLC-MS/MS using an AccQ-Tag Ultra 100 mm \times 2.1 mm (1.7 μm particle size) column (Waters). A binary gradient system of water-eluent A (10:1, v/v) (AccQ-Tag, Waters) and 100% eluent B (AccQ-Tag, Waters), was used. Elution of the analytes was achieved by ramping the percentage of eluent B from 0.1 to 90.0 in approx. 9.5 min using a combination of both linear and convex profiles. The flow-rate was 0.7 ml/min and the column temperature was maintained at 60°C. After each injection, the injection needle was washed with 200 μl 95:5 v/v ACN:water and subsequently with 600 μl 5:95 v/v ACN:water.

The Quattro Premier XE was used in the positive-ion electrospray mode and all analytes were monitored in Selective Reaction Monitoring (SRM) using nominal mass resolution; the width of the isolation/fragmentation window was set to 0.7 Da. All target compounds were

monitored via the transition from the protonated molecule of the AccQ-Tag derivative to the common fragment at m/z 171. Collision energy and collision gas (Ar) pressure were 22 eV and 2.5 mbar, respectively. The identities of all compounds were confirmed by high resolution MS and identical retention times as authentic standards (data not shown). The acquisition run was divided into six time segments in order to decrease the number of simultaneous SRM transitions. All samples were analyzed in duplicate, and measurement order was randomized.

Acquired data were evaluated using Quanlynx software (Waters), by integration of assigned SRM peaks and normalization using proper internal standards. For analysis of amino acids, their $^{13}\text{C}^{15}\text{N}$ -labeled analogs were used. For other amines—the closest-eluting internal standard was employed. Resulting relative responses from duplicate injections were averaged after visual inspection.

2.4 GC-MS method

The GC-MS platform used in this study requires 30 μl of rat CSF for sufficient sensitivity and coverage. Because only 10 μl CSF per rat was available, samples were pooled per three. This resulted in 30 μl pooled rat CSF samples and group sizes of 5 (groups H₁₀, H₁₄, CFA₁₀, CFA₁₄, EAE₁₀) and 3 (group EAE₁₄, limited number of samples available, see Section 2.2). The samples (30 μl) were deproteinized by adding 250 μl methanol and subsequently centrifuged for 10 min at 11800 rpm. The supernatant was dried under N_2 followed by derivatization with methyl-*N*-(trimethylsilyl)-trifluoroacetamide (MSTFA) in pyridine similar to Koek et al. (2006). During the different steps in the sample work-up, i.e. prior to deproteinization, derivatization and injection, different (deuterated) internal standards were added at a level of approx. 20 ng/ μl . The end volume was 45 and 1 μl aliquots of the derivatized samples were injected in splitless mode on a HP5-MS 30 m \times 0.25 mm \times 0.25 μm capillary column (Agilent Technologies, USA) using a temperature gradient from 70 to 320°C at a rate of 5°C/min. GC-MS analysis was performed using an Agilent 6890 gas chromatograph coupled to an Agilent 5973 mass selective detector (Agilent Technologies, USA). Detection was carried out using MS detection in electron impact mode and full scan monitoring mode (m/z 15–800). The electron impact for the generation of ions was 70 eV. Samples were analyzed in duplicate.

Data-pre-processing was carried out by composing target lists of peaks detected in the samples based on retention time and mass spectra and these peaks were integrated for all samples. All peak areas were subsequently normalized using internal standards. The resulting target lists were used for further statistical analysis. Identities were assigned based on the presence of identical mass spectra in an

in-house database based on authentic standards (data not shown).

3 Data analysis

The significance of MBP treatment for all metabolites was assessed by linear modeling (Draper and Smith 1998). Three models were fitted for each metabolite. The first global model (Eq. 1) includes all data for each metabolite:

$$y = \beta_0 + \beta_1 \text{weight}_{\text{day}0} + \beta_2 \text{CFA} + \beta_3 \text{MBP} + \beta_4 \text{time} + \beta_5 \text{CFA} \times \text{time} + \beta_6 \text{MBP} \times \text{time} \quad (1)$$

in which y = metabolite response; CFA = CFA injected (1 for CFA and EAE groups, otherwise 0); MBP = MBP injected (1 for EAE groups, otherwise 0); $\beta_0 \dots \beta_6$ = model coefficients; time = number of days since start of the experiment (10 or 14); $\text{weight}_{\text{day}0}$ = weight at day 0 (for LC-MS, individual rat LC-MS; for GC-MS, average of rats in pooled sample) [g].

To obtain a higher confidence, two additional single-day models were fitted for the samples collected on day 10 and day 14, respectively (Eq. 2):

$$y_{\text{day}X} = \alpha_0 + \alpha_1 \text{weight}_{\text{day}0} + \alpha_2 \text{CFA} + \alpha_3 \text{MBP} \quad (2)$$

in which (other symbols are explained above) $y_{\text{day}X}$ = metabolite response at day X (X is 10 or 14) and $\alpha_0 \dots \alpha_3$ = model coefficients.

For all three models, stepwise linear regression (Massart et al. 1997) was used to remove non-significant terms. The significance of the regression coefficients in the final models was obtained from a t test ($H_0: \alpha_i = 0$, $H_1: \alpha_i \neq 0$ or $H_0: \beta_i = 0$, $H_1: \beta_i \neq 0$).

A significant EAE effect in an individual single day model is present when there is a significant α_3 . However, here a distinction between a time dependent and a time independent effect cannot be made. For the combined model, a time-dependent effect is given by a significant β_6 and a time-independent effect is given by a significant β_3 .

We distinguish between three effects: early stage EAE, full stage EAE and EAE progression. For an effect to be significant it must be present in both the combined model and at least one single day model, otherwise results are considered to be inconclusive.

A significant early stage EAE effect is reported when a significant α_3 in the day 10 model is observed together with a significant β_3 and/or β_6 in the combined model. A significant α_3 in the day 14 model together with a significant β_3 and/or β_6 in the combined model indicates full stage EAE. An EAE progression effect is reported when a significant β_6 in the combined model is observed in correlation with a significant α_3 in at least one of the single day models.

Fold changes are obtained by taking ratios between average model calculated metabolite responses per treatment group. The fold changes for the onset ($\text{EAE}_{10}/\text{CFA}_{10}$) and peak ($\text{EAE}_{14}/\text{CFA}_{14}$) of the disease are calculated from the respective single day model results (Eq. 2). Fold changes for EAE progression ($\text{EAE}_{14}/\text{EAE}_{10}$) are obtained from the global model results (Eq. 1).

4 Results

Figure 1 shows the progression of animal growth (weight, left axis) for all experimental groups. For animals from EAE_{14} , progression of EAE is also shown (neurological scores, right axis). The weight change during the course of the experiment is dependent on multiple factors and therefore difficult to use as quantitative measure in the data analysis. Nevertheless, it accounts for the overall well-being of the animal. Because of the fast growth of animals (4–6 g per day), the complex treatment and use of two sampling time-points, growth of the animals may affect the metabolic profile. In addition, after the onset of the disease, animals from EAE group started losing weight and this decrease is correlated with the increase of neurological scores (see Fig. 1). As a consequence, the weight of the animals from EAE_{14} group was significantly lower than from all the other groups. The exact cause for this effect is not certain. It is possible that progressing paralysis impaired the animals ability to feed themselves, however animals were able to eat and drink while lying. The degree to which weight loss influences the volume of CSF and concentration of metabolites is hard to access.

Principal component analysis (PCA) was applied for preliminary visual inspection of the metabolite profiles of

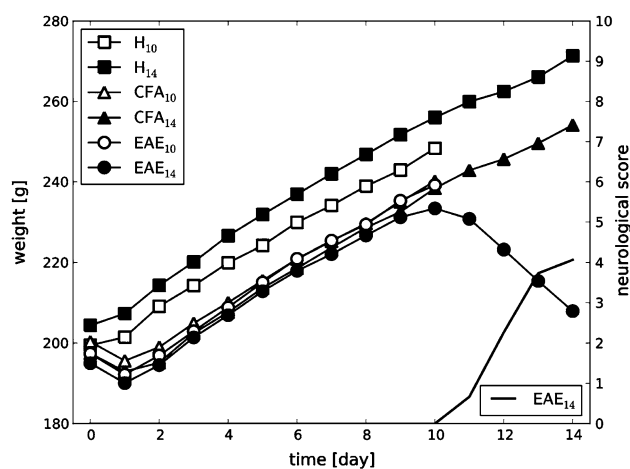


Fig. 1 Weight trends (left axis) and neurological scores (right axis) during the course of the animal experiment. Standard deviation of weights within each group was in range of 8–12 g, bars not shown for sake of clarity

the CSF samples belonging to the different groups (Figs. 2, 3). Prior to PCA, each metabolite was scaled to zero mean and unit variance. Clear separation between the full-stage EAE group (EAE₁₄) and the other groups is observed for both platforms. The GC-MS data (Fig. 3) also show partial separation of early stage EAE samples (group EAE₁₀). For LC-MS (Fig. 2) this separation is not observed although some separation can be seen in higher principal components (see Figure S1 in supplementary material).

Table 1 summarizes the LC-MS linear modeling results. The table also indicates overlapping GC-MS targets and where the GC-MS linear modeling results confirm effect

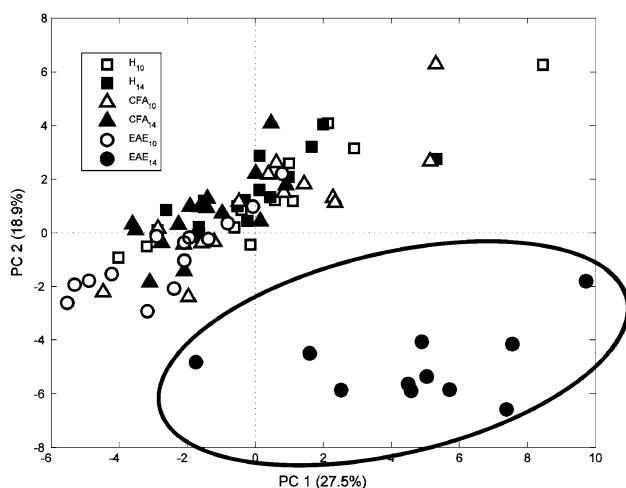


Fig. 2 PCA scores plot of LC-MS data. *Filled symbols* represent the day 14 samples while the *open symbols* represent the day 10 samples. Clear separation between samples from group with full stage EAE (group F, enclosed in ellipse) is observed

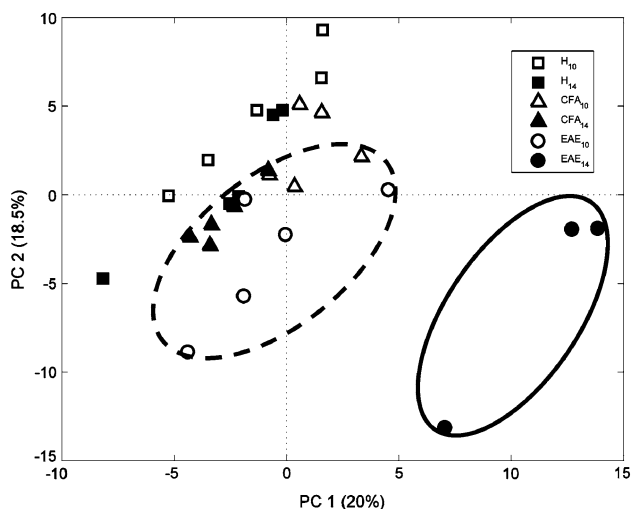


Fig. 3 PCA scores plot of GC-MS data. *Filled symbols* represent the day 14 samples while the *open symbols* represent the day 10 samples. Ellipses show grouping of samples from EAE-affected animals—early stage EAE (group E, partially separated as indicated by *dashed line*) and full stage of EAE (group F, *solid line*)

directionality. Although directionality is not always confirmed by linear modeling, visual inspection of the GC-MS data indicates agreement. There are no cases where LC-MS and GC-MS effects have opposite direction. The smaller groups in GC-MS as a result of sample pooling restrict the ability to draw unambiguously reliable biological conclusions based on that platform alone. Therefore, GC-MS linear modeling results are supplied as supplementary material.

Significant changes of metabolite levels detected by linear models were verified by pair wise comparison using double-sided *t* tests and visually inspected by boxplot per molecule. Figure 4 below shows a boxplot presenting concentration changes of putrescine—the metabolite that showed biggest fold-change between the experimental groups.

5 Discussion

The design of the biological experiments, with three treatments groups—healthy controls, a CFA group with animals subjected to peripheral inflammation only and a full EAE treatment, allowed for separation of the concentration changes caused by EAE from possible variations due to adjuvant injection, including variations due to animal growth or peripheral inflammation.

Several significant changes in concentrations of metabolites both at the onset and on the peak of the disease were detected. Dissimilar patterns of changes observed on both time points may suggest activation of different metabolic pathways in the early and late stage of the disease. The early-stage EAE samples, taken on day 10 post inoculation resemble the moment of maximal CNS infiltration by blood monocytes and T-cells, however, at this moment no negative signs on health status are observed and animals do not have any neurological scores. Metabolite level changes in the early stage of the disease may be caused by processes related to the development of EAE and disruption of the blood-CSF barrier.

The full-stage EAE samples are taken on day 14, at the peak of the disease, when the paralysis of the animals is most severe, which is expressed in maximum neurological scores (see Fig. 1). The EAE model employed in this study involves spontaneous recovery of animals. In fact, due to the slightly heterogeneous course of the disease, 2 out of 15 animals from the EAE₁₄ group had neurological scores which had already decreased relative to the previous day. Therefore, one can assume that some metabolites observed as significantly regulated in this sample series might be connected to pathological processes involved in EAE progression or recovery. The observed weight loss of EAE₁₄ animals poses a difficult challenge in interpretation

Table 1 Statistically significant concentration ratios as a result of MBP treatment for compounds detected by LC–MS

Name	HMDB ID	Pubchem CID	EAE onset	Peak of EAE	EAE progression
1-Methylhistidine	HMDB00001	10225185		3.6 ⁺⁺	1.2 ⁺⁺
3-Methoxytyramine	HMDB00022	3885186			
3-Methoxytyrosine	HMDB01434	6385645			
3-Methylhistidine	HMDB00479	15171160			
Beta-alanine	HMDB00056	11113405			
Citrulline	HMDB00904	11532235	0.91 ⁻	0.62 ⁻	0.69 ⁻
Cyclic GMP	HMDB01314	24316			
Dopamine	HMDB00073	6517			
Epinephrine	HMDB00068	8144253			
Gamma-aminobutyric acid	HMDB00112	119		3.3 ⁺⁺	2.7 ⁺⁺
Glycine ^a	HMDB00123	750			
Histamine	HMDB00870	10524836			
Homo-L-arginine	HMDB00670	5030		2.6 ⁺⁺	2.2 ⁺⁺
Homocysteine	HMDB00742	8144236			
L-Alanine ^a	HMDB00161	5950	0.87 ^{-*}	0.78 ⁻	0.93 ⁻
L-Alpha-aminobutyric acid	HMDB00452	10217858		1.9 ⁺⁺	1.9 ⁺⁺
L-Arginine	HMDB00517	10318557	0.82 ⁻		1.2 ⁺⁺
L-Asparagine ^a	HMDB00168	6267	0.90 ^{-*}	1.2 ^{+++*}	1.2 ^{+++*}
L-Aspartic acid	HMDB00191	3351			
L-Glutamic acid ^a	HMDB00148	33032		0.67 ⁻	0.89 ⁻
L-Glutamine ^a	HMDB00641	5961	0.86 ⁻	1.2 ⁺⁺	1.4 ⁺⁺
L-Histidine	HMDB00177	8023160		1.4 ⁺⁺	1.6 ⁺⁺
L-Isoleucine ^a	HMDB00172	791	0.83 ⁻	1.2 ⁺⁺	1.2 ⁺⁺
L-Kynurenine	HMDB00684	11375672			
L-Leucine ^a	HMDB00687	6106	0.87 ⁻	1.3 ⁺⁺	1.3 ⁺⁺
L-Lysine ^a	HMDB00182	5962		1.9 ⁺⁺	1.7 ⁺⁺
L-Methionine ^a	HMDB00696	6137	0.79 ^{-*}		
L-Phenyl alanine ^a	HMDB00159	6140	0.86 ^{-*}	1.3 ^{+++*}	1.4 ^{+++*}
L-Proline ^a	HMDB00162	145742			
L-Serine ^a	HMDB00187	5951	0.90 ^{-*}		
L-Threonine ^a	HMDB00167	6288		1.8 ^{+++*}	2.1 ^{+++*}
L-Tryptophan	HMDB00929	6305	0.88 ⁻	1.4 ⁺⁺	1.6 ⁺⁺
L-Tyrosine	HMDB00158	817487	0.82 ⁻		
L-Valinel	HMDB00883	1182	0.84 ⁻	1.1 ⁺⁺	1.2 ⁺⁺
N6,N6,N6-Trimethyl-L-lysine	HMDB01325	6542		1.5 ⁺⁺	1.7 ⁺⁺
O-Phosphoethanolamine ^a	HMDB00224	1015	1.1 ⁺	2.5 ^{+++*}	2.1 ^{+++*}
Ornithinel	HMDB00214	6262	0.79 ⁻		
Putrescine	HMDB01414	17436307		14 ⁺⁺	13 ⁺⁺
Taurinel	HMDB00251	1123	1.1 ⁺	1.5 ⁺⁺	1.3 ⁺⁺

Single and double symbols denote respectively 95 and 99% significance levels of the observed EAE effects (– denotes decrease, + denotes increase)

EAE onset = EAE₁₀/CFA₁₀, Peak of EAE = EAE₁₄/CFA₁₄, EAE progression = EAE₁₄/EAE₁₀. See Section 3 for details

* Effect directionality confirmed by GC–MS

^a Compounds that were also measured by GC–MS

of observed changes. It was shown in the literature that weight loss and dietary restriction may cause changes in metabolite profiles in body fluids (Bollard et al. 2005). However, it is unknown how these changes affect CSF

metabolic profile. For that reason the brief interpretation of biological relevance of observed changes presented below is mostly limited to compounds involved in processes previously associated with MScl and EAE.

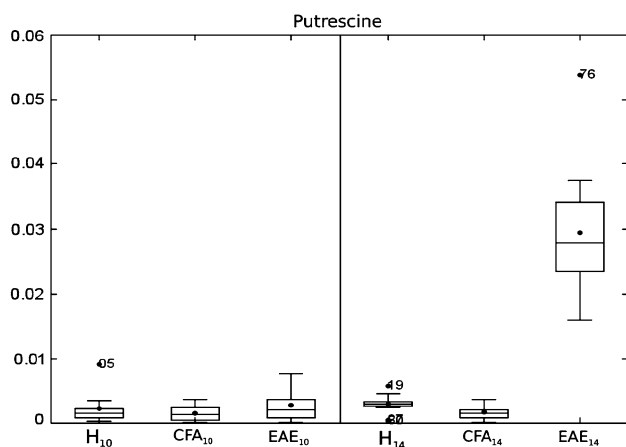


Fig. 4 Box plot showing concentration of putrescine in all experimental groups. Note significant increase in concentration in EAE₁₄ group. The outlying rat 76, with the highest level of putrescine, started to recover during the last day prior to sampling. See text for discussion

Several metabolites targeted in this study and found significantly up/down-regulated were previously associated with molecular processes interconnected with development of MS and EAE. Glutamic acid (glutamate), glutamine, gamma-aminobutyric acid (GABA), asparagine and taurine are involved in excitotoxicity and energy metabolism. Arginine and citrulline play a key role in NO synthesis. Arginine, ornithine and putrescine are involved in polyamine synthesis. Alanine and branched-chain amino acids (valine, leucine, isoleucine) are involved in energy metabolism. See Table 2 for overview.

5.1 Excitotoxicity

L-glutamic acid (glutamate) is a ubiquitous neurotransmitter with several identified receptors and transport proteins both in neural and glial cells (Danbolt 2001). Over-stimulation of glutamate receptors may cause cell death due to

Table 2 Overview of most important biological processes interconnected with significantly regulated changes in metabolome detected in this study

Molecular process	Related significantly regulated compounds
Excitotoxicity	Glutamic acid, glutamine, asparagine, gamma-aminobutyric acid
Peroxonitration	Arginine, citrulline
Polyamine synthesis	Arginine, ornithine, putrescine
Oxidative stress	Taurine
Energy metabolism	Glutamine, alanine, BCAA (leucine, isoleucine, valine)
Lipid metabolism	Phosphoethanolamine

excitotoxicity. Indeed, elevated levels of CSF glutamate were reported in clinical cases of multiple sclerosis (Sarchielli et al. 2003). Contrary to previous reports, as shown in Table 1, the level of glutamic acid in this study shows a statistically significant decrease in concentration at the peak of the disease, while no significant change is observed at the early stage. However, the glutamine, which is closely interconnected with glutamate through glutamine-glutamate cycle in neurons and astrocytes, shows down-regulation at the onset and up-regulation with full stage EAE. Conversion of glutamate into glutamine by glutamine synthetase (GS) enzyme localized in astrocytes is a key process protecting neurons from ammonia toxicity (Norenberg and Martinez-Hernandez 1979) and the only pathway of ammonia disposal due to the lack of complete urea cycle in CNS (Wiesinger 2007). Available evidence shows up-regulation of GS in astrocytes present in demyelinating lesions as assessed in a study of post mortem brain tissue of MS patients (Newcombe et al. 2008). However, a similar study performed in MBP-induced mouse EAE shows down-regulation of this enzyme (Hardin-Pouzet et al. 1997).

At the peak of the disease we observe a significant gamma-aminobutyric acid (GABA) increase. GABA is synthesized from glutamate by glutamate decarboxylase. It was shown that GABA, an inhibitory neurotransmitter, may attenuate glutamate-induced excitotoxicity (Ohkuma et al. 1994). In our study we observe significant increase in concentration of another inhibitory neurotransmitter, taurine, which was also shown to be protective against excitotoxicity (El Idrissi and Trenkner 1999).

It should also be emphasized that glutamate, besides having a profound role as a neurotransmitter in CNS, is one of the key metabolites in energy metabolism of neurons, glia and immune cells (Newsholme et al. 1999). It is possible that the global CSF levels of glutamine and glutamate involved in energy metabolism dominate over local high and excitotoxic concentrations in the most affected regions of brain and spinal cord. The observed discrepancy between available results on glutamate up- and down-regulation in EAE/MS suggests it may be involved in multiple different molecular processes associated with neuroinflammation and neurodegeneration.

5.2 Cytotoxicity interconnected with peroxynitrylation

Peroxonitrite anion (ONOO⁻) is a very reactive oxidizing agent, capable of inducing cell death through multiple pathways (Szabó et al. 2007). It emerges in the reaction between nitric oxide, produced mainly by inductive nitric oxide synthetase (iNOS) in activated immune cells and microglia, and the free radical superoxide O₂⁻, coming from oxidative phosphorylation cycle in mitochondria.

Currently available evidence suggests, besides promotion of peroxynitrite synthesis, that NO plays a complex regulatory role in mediating the immune response (van der Veen et al. 1997). Numerous reports suggest activity of peroxynitrite in active lesions in MScl (Smith and Lassmann 2002), as well as in EAE (van der Veen et al. 1997).

In our study we observe significant down-regulation of arginine, the main substrate for NO synthesis during the early stage of EAE. This effect may be interconnected with intense production of NO by cytotoxic T-cells, macrophages and activated microglia during development of neuroinflammation. However, the exact role of NO in EAE and MScl development remains unclear. Available reports show that inhibition of NO synthesis may attenuate (Ding et al. 1998) or enhance (Zielasek et al. 1995) EAE.

Interestingly, a second product of NO synthesis, citrulline, is also significantly down-regulated in the early stage of EAE, while one could expect increased production of citrulline linked to increased NO synthesis. However, immune and CNS cells are able to re-synthesize arginine in the so-called arginine-NO cycle (see Fig. 5, solid line). This cycle can be considered as a shortcut of the urea cycle (Fig. 5, dashed line), which due to the lack of ornithine carbamoyltransferase (OTC) is not complete in the CNS

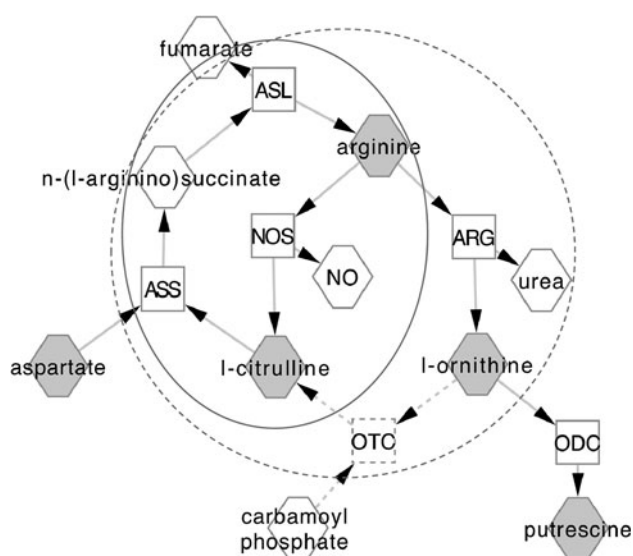


Fig. 5 Overview of pathways of arginine metabolism in CNS. Hexagons depict metabolites and squares—reactions. Compounds measured in our study are marked in grey. Ornithine transcarbamoylase (OTC), argininosuccinate synthetase (ASS), argininosuccinate lyase (ASL) and arginase (ARG) are enzymes in the urea cycle (dashed circle), however OTC (dashed) is not expressed in CNS. Nitric oxide synthetase (NOS) is used for synthesis of nitric oxide and part of arginine-NO cycle (solid ellipsis). Ornithine decarboxylase (ODC) produces putrescine that is later used in synthesis of other polyamines. This figure was generated using Cytoscape (www.cytoscape.org)

(Wiesinger 2001). It was demonstrated that arginine deficiency does not inhibit NO synthesis by T-cells, which under such circumstances are able to increase uptake of citrulline and up-regulate enzymes responsible for arginine synthesis (Bansal et al. 2004). Due to the involvement of arginine in other reactions, the citrulline-NO cycle does not operate in a stoichiometric manner, resulting in simultaneous decrease of arginine and citrulline levels.

It should be also noted that the most significant alternative reaction of arginine utilization is the synthesis of ornithine by the enzyme arginase (ARG). This reaction is known to take part in regulating NO synthesis by reducing the amount of available arginine (Bansal and Ochoa 2003). In the early stage of EAE we observe a decrease in the concentration of ornithine, supporting the hypothesis that arginine is probably being utilized by NO synthesis.

5.3 Polyamine synthesis

During the peak of EAE, arginine levels do not differ from controls, while citrulline levels continue to decrease. This may be explained by the reduction of NO synthesis interconnected with continued activity of other citrulline-NO cycle enzymes. At the same time we observe up-regulation of products of an alternative pathway of arginine utilization. The ornithine levels return to their normal states after significant decreases during the EAE onset, and this correlates with the significant 20-fold increase of putrescine levels, synthesised from ornithine by ornithine decarboxylase (see Fig. 4). These results may suggest a switch in arginine metabolism from nitric oxide production towards the synthesis of ornithine and further to polyamine synthesis, which could be associated with compensatory anti-inflammatory response and recovery. Interestingly, the rat with the highest observed level of putrescine is a clear outlier from the rest of the group (animal 76 on Fig. 4) and is one of two animals in the group that showed a neurological score decrease on the last day of experiment.

Putrescine was reported to be up-regulated in EAE (Bolton and Paul 2006), however this change was associated with disease progression rather than recovery mechanisms. On the other hand, the beneficial effect of increased polyamine synthesis on post-injury recovery of CNS was demonstrated in literature (Gilad et al. 1996; Cai et al. 2002). Available reports show the potential of putrescine to block NMDA glutamate receptors (Williams 1997) and therefore could possibly attenuate excitotoxic effects of glutamate.

It was postulated previously that over the course of inflammation, metabolism of arginine switches from NO synthesis in the early stage to arginine utilization in polyamine synthesis during tissue repair and wound healing (Nelin et al. 2007).

5.4 Protection from oxidative stress

It was shown that antioxidants, such as uric acid, inhibit inflammation in EAE (Hooper et al. 2000). The inhibitory neurotransmitter taurine, observed as up-regulated in our study, is also known for its antioxidant and anti-inflammatory activity (Li et al. 2007). Levels of taurine increase over the course of EAE, suggesting that they may play a role in protection and recovery mechanisms. As the neurotoxicity of peroxyacetyl nitrate might be dependent on the availability of superoxide rather than nitric oxide alone, it was suggested that MScl may be in fact connected with a malfunction of mitochondria (Mao and Reddy 2010) or imbalance of ATP synthesis and energy metabolism (Cadoux-Hudson et al. 1991; Amorini et al. 2009).

5.5 Energy metabolism

Besides changes discussed above, we also observe other changes in the metabolome that cannot be clearly connected to already established hypotheses of MScl/EAE mechanisms. In the early stage of the EAE we observe decreased levels of alanine and branched-chain amino-acids (BCAA: leucine, isoleucine and valine). Alanine and BCAAs are known to be utilized as a source for pyruvate for energy metabolism or de novo synthesis of macromolecules within neural (Hutson et al. 2007) and immune cells (Li et al. 2007). As the onset of EAE is associated with maximum infiltration of the CNS by blood monocytes and T-cells, the observed decrease of BCAAs and alanine may suggest these metabolites are utilized for energy metabolism by invading cells. Alternatively, pro-inflammatory cytokines released during EAE development may cause changes in energy metabolism of native CNS cells.

5.6 Phospholipid metabolism

In the full stage EAE, among other changes, we observe a significant increase of *O*-phosphoethanolamine concentration, which is an important intermediate in phospholipid metabolism. Wheeler et al. (2008) reported changes in lipid contents in normal appearing white and grey matter of MScl patients, suggesting changes in lipid metabolism including increased sphingolipid turnover and phospholipid synthesis. The detected increase of *O*-phosphoethanolamine might be interconnected with these processes.

6 Conclusions and future prospects

A targeted metabolomic approach of metabolites containing amino groups was applied to study changes in CNS metabolism in a MScl rat model. The obtained results

showed significant changes in metabolic processes during the onset and progression of EAE. Excessive nitric oxide production along with changes in energy metabolism appear to play a key role in the development of the EAE, while a switch from arginine metabolism to polyamine synthesis may be associated with processes involved in spontaneous recovery of affected animals. Further research is required to confirm these hypotheses.

Results obtained in this study are partially in agreement with established knowledge on EAE and multiple sclerosis. However, in some cases we observe changes conflicting with previously published results. It should be noted that the vast majority of existing results were obtained in different experiments, executed in different paradigms, investigating similar, however still distinct biological conditions. Established EAE models differ from each other and still they do not cover all aspects of multiple sclerosis (Lassmann 2007). The ability to simultaneously measure a wide range of compounds is advantageous in systems biology approaches, like the one presented here. The use of a common experiment to probe multiple pathways in a biological system yields a chance for obtaining more comprehensive and coherent picture of molecular mechanisms involved.

Our results prove that metabolomics provides useful insights into the mechanisms underlying biological processes in the onset and development of multiple sclerosis using a rat model. High sensitivity and a wide range of metabolites were covered by the present analytical platforms, which allowed for a reliable screening of potential changes in CNS metabolism. In contrast to untargeted approaches, our LC/GC-MS analysis focuses on the measurement of well defined and confidently identified components. This allowed a more accurate description of the potential molecular mechanisms involved.

Acknowledgments Authors would like to acknowledge Frans van der Kloet (LACDR) and Siem Heisterkamp (MSD) for batch design for LC-MS and GC-MS experiments, respectively. We also thank Amy Harms and Vanessa Gonzalez (both LACDR) for reading and commenting on this manuscript. This study was financially supported by Top Institute Pharma project D4-102. This study was supported by the research program of the Netherlands Metabolomics Centre (NMC), which is a part of The Netherlands Genomics Initiative/Netherlands Organization for Scientific Research.

Open Access This article is distributed under the terms of the Creative Commons Attribution Noncommercial License which permits any noncommercial use, distribution, and reproduction in any medium, provided the original author(s) and source are credited.

References

- Amorini, A. M., Petzold, A., Tavazzi, B., et al. (2009). Increase of uric acid and purine compounds in biological fluids of multiple sclerosis patients. *Clinical Biochemistry*, 42, 1001–1006.

- Bansal, V., & Ochoa, J. B. (2003). Arginine availability, arginase, and the immune response. *Current Opinion in Clinical Nutrition and Metabolic Care*, 6, 223–228.
- Bansal, V., Rodriguez, P., Wu, G., et al. (2004). Citrulline can preserve proliferation and prevent the loss of CD3 zeta chain under conditions of low arginine. *Journal of Parenteral and Enteral Nutrition*, 28, 423–430.
- Bollard, M. E., Stanley, E. G., Lindon, J. C., Nicholson, J. K., & Holmes, E. (2005). NMR-based metabolomic approaches for evaluating physiological influences on biofluid composition. *NMR in Biomedicine*, 18, 143–162.
- Bolton, C., & Paul, C. (2006). Glutamate receptors in neuroinflammatory demyelinating disease. *Mediators of Inflammation*, 2006, 93684.
- Cadoux-Hudson, T. A., Kermodé, A., Rajagopalan, B., et al. (1991). Biochemical changes within a multiple sclerosis plaque in vivo. *Journal of Neurology, Neurosurgery and Psychiatry*, 54, 1004–1006.
- Cai, D., Deng, K., Mellado, W., Lee, J., Ratan, R. R., & Filbin, M. T. (2002). Arginase I and polyamines act downstream from cyclic AMP in overcoming inhibition of axonal growth MAG and myelin in vitro. *Neuron*, 35, 711–719.
- Carrasco-Pancorbo, A., Nevedomskaya, E., Arthen-Engeland, T., et al. (2009). Gas chromatography/atmospheric pressure chemical ionization-time of flight mass spectrometry: analytical validation and applicability to metabolic profiling. *Analytical Chemistry*, 81, 10071–10079.
- Crews, B., Wikoff, W. R., Patti, G. J., et al. (2009). Variability analysis of human plasma and cerebral spinal fluid reveals statistical significance of changes in mass spectrometry-based metabolomics data. *Analytical Chemistry*, 81, 8538–8544.
- Danbolt, N. C. (2001). Glutamate uptake. *Progress in Neurobiology*, 65, 1–105.
- Ding, M., Zhang, M., Wong, J. L., Rogers, N. E., Ignarro, L. J., & Voskuhl, R. R. (1998). Antisense knockdown of inducible nitric oxide synthase inhibits induction of experimental autoimmune encephalomyelitis in SJL/J mice. *Journal of Immunology*, 160, 2560–2564.
- Draper, N. R., & Smith, H. (1998). *Applied regression analysis*. New York: John Wiley & Sons.
- El Idrissi, A., & Trenkner, E. (1999). Growth factors and taurine protect against excitotoxicity by stabilizing calcium homeostasis and energy metabolism. *Journal of Neuroscience*, 19, 9459–9468.
- Gilad, V. H., Tetzlaff, W. G., Rabey, J. M., & Gilad, G. M. (1996). Accelerated recovery following polyamines and aminoguanidine treatment after facial nerve injury in rats. *Brain Research*, 724, 141–144.
- Hardin-Pouzet, H., Krakowski, M., Bourbonnière, L., Didier-Bazes, M., Tran, E., & Owens, T. (1997). Glutamate metabolism is down-regulated in astrocytes during experimental allergic encephalomyelitis. *Glia*, 20, 79–85.
- Hendriks, J. J., Alblas, J., van der Pol, S. M., van Tol, E. A., Dijkstra, C. D., & de Vries, H. E. (2004). Flavonoids influence monocytic GTPase activity and are protective in experimental allergic encephalitis. *Journal of Experimental Medicine*, 200, 1667–1672.
- Hooper, D. C., Scott, G. S., Zborek, A., et al. (2000). Uric acid, a peroxynitrite scavenger, inhibits CNS inflammation, blood-CNS barrier permeability changes, and tissue damage in a mouse model of multiple sclerosis. *FASEB J*, 14, 691–698.
- Hutson, S. M., Sweatt, A. J., & LaNoue, K. F. (2007). Branched Chain Amino Acids (BCAAs) in Brain. In S. S. Oja, P. Saransaari, & A. Schousboe (Eds.), *Handbook of neurochemistry and molecular neurobiology: amino acids and peptides in the nervous system* (pp. 117–131). Springer-Verlag: Berlin Heidelberg.
- Koek, M. M., Muilwijk, B., van der Werf, M. J., & Hankemeier, T. (2006). Microbial metabolomics with gas chromatography/mass spectrometry. *Analytical Chemistry*, 78, 1272–1281.
- Lassmann, H. (2007). Multiple Sclerosis and Autoimmune Encephalomyelitis. In A. Lajtha, M. B. H. Youdim, P. Riederer, S. A. Mandel, L. Battistin, & H. Lassmann (Eds.), *Handbook of neurochemistry and molecular neurobiology* (pp. 373–404). US: Springer.
- Li, P., Yin, Y. L., Li, D., Kim, S. W., & Wu, G. (2007). Amino acids and immune function. *British Journal of Nutrition*, 98, 237–252.
- Mao, P., & Reddy, P. H. (2010). Is multiple sclerosis a mitochondrial disease? *Biochimica et Biophysica Acta*, 1802, 66–79.
- Massart, D. L., Vandeginste, B. M. G., Buydens, L. M. C., de Jong, S., Lewi, P. J., & Smeyers-Verbeke, J. (1997). *Multiple and Polynomial Regression. Handbook of chemometrics and quality metrics Part A* (pp. 263–303). Amsterdam: Elsevier.
- Myint, K. T., Aoshima, K., Tanaka, S., Nakamura, T., & Oda, Y. (2009). Quantitative profiling of polar cationic metabolites in human cerebrospinal fluid by reversed-phase nanoliquid chromatography/mass spectrometry. *Analytical Chemistry*, 81, 1121–1129.
- Nelin, L. D., Wang, X., Zhao, Q., et al. (2007). MKP-1 switches arginine metabolism from nitric oxide synthase to arginase following endotoxin challenge. *American Journal of Physiology Cell Physiology*, 293, C632–C640.
- Newcombe, J., Uddin, A., Dove, R., et al. (2008). Glutamate receptor expression in multiple sclerosis lesions. *Brain Pathology*, 18, 52–61.
- Newsholme, P., Curi, R., Pithon Curi, T. C., Murphy, C. J., Garcia, C., & Pires de Melo, M. (1999). Glutamine metabolism by lymphocytes, macrophages, and neutrophils: its importance in health and disease. *Journal of Nutritional Biochemistry*, 10, 316–324.
- Norenberg, M. D., & Martinez-Hernandez, A. (1979). Fine structural localization of glutamine synthetase in astrocytes of rat brain. *Brain Research*, 161, 303–310.
- Ohkuma, S., Chen, S. H., Katsura, M., Chen, D. Z., & Kuriyama, K. (1994). Muscimol prevents neuronal injury induced by NMDA. *Japanese Journal of Pharmacology*, 64, 125–128.
- Sarchielli, P., Greco, L., Floridi, A., & Gallai, V. (2003). Excitatory amino acids and multiple sclerosis: Evidence from cerebrospinal fluid. *Archives of Neurology*, 60, 1082–1088.
- Smith, K. J., & Lassmann, H. (2002). The role of nitric oxide in multiple sclerosis. *Lancet Neurology*, 1, 232–241.
- Szabó, C., Ischiropoulos, H., & Radi, R. (2007). Peroxynitrite: Biochemistry, pathophysiology and development of therapeutics. *Nature Reviews Drug Discovery*, 6, 662–680.
- van der Veen, R. C., Hinton, D. R., Incardonna, F., & Hofman, F. M. (1997). Extensive peroxynitrite activity during progressive stages of central nervous system inflammation. *Journal of Neuroimmunology*, 77, 1–7.
- Wheeler, D., Bandaru, V. V. R., Calabresi, P. A., Nath, A., & Haughey, N. J. (2008). A defect of sphingolipid metabolism modifies the properties of normal appearing white matter in multiple sclerosis. *Brain*, 131, 3092–3102.
- Wiesinger, H. (2001). Arginine metabolism and the synthesis of nitric oxide in the nervous system. *Progress in Neurobiology*, 64, 365–391.
- Wiesinger, H. (2007). Arginine, Citrulline, and Ornithine. In S. S. Oja, P. Saransaari, & A. Schousboe (Eds.), *Handbook of neurochemistry and molecular neurobiology: Amino Acids and peptides in the nervous system* (pp. 99–115). Berlin Heidelberg: Springer-Verlag.
- Williams, K. (1997). Modulation and block of ion channels: a new biology of polyamines. *Cellular Signalling*, 9, 1–13.
- Wishart, D. S., Lewis, M. J., Morrissey, J. A., et al. (2008). The human cerebrospinal fluid metabolome. *Journal of Chromatography B*, 871, 164–173.
- Wuolikainen, A., Hedenström, M., Moritz, T., Marklund, S. L., Antti, H., & Andersen, P. M. (2009). Optimization of procedures for

collecting and storing of CSF for studying the metabolome in ALS. *Amyotrophic Lateral Sclerosis*, *10*, 229–236.

Zielasek, J., Jung, S., Gold, R., Liew, F. Y., Toyka, K. V., & Hartung, H. P. (1995). Administration of nitric oxide synthase inhibitors

in experimental autoimmune neuritis and experimental autoimmune encephalomyelitis. *Journal of Neuroimmunology*, *58*, 81–88.